

ORIGINAL RESEARCH



Bovine herpesvirus 4-based vector delivering the full length xCT DNA efficiently protects mice from mammary cancer metastases by targeting cancer stem cells

Gaetano Donofrio ^a, Giulia Tebaldi^a, Stefania Lanzardo^b, Roberto Ruii ^b, Elisabetta Bolli ^b, Andrea Ballatore^b, Valeria Rolih ^b, Francesca Macchi^a, Laura Conti ^{b*}, and Federica Cavallo ^{b*}

^aDepartment of Medical Veterinary Science, Università degli Studi di Parma, Parma, Italy; ^bDepartment of Molecular Biotechnology and Health Sciences, Molecular Biotechnology Center, Università degli Studi di Torino, Torino, Italy

ABSTRACT

Despite marked advancements in its treatment, breast cancer is still the second leading cause of cancer death in women, due to relapses and distal metastases. Breast cancer stem cells (CSCs), are a cellular reservoir for recurrence, metastatic evolution and disease progression, making the development of novel therapeutics that target CSCs, and thereby inhibit metastases, an urgent need. We have previously demonstrated that the cystine-glutamate antiporter xCT (SLC7A11), a protein that was shown to be overexpressed in mammary CSCs and that plays a key role in the maintenance of their redox balance, self-renewal and resistance to chemotherapy, is a potential target for mammary cancer immunotherapy. This paper reports on the development of an anti-xCT viral vaccine that is based on the bovine herpesvirus 4 (BoHV-4) vector, which we have previously showed to be a safe vaccine that can transduce cells *in vivo* and confer immunogenicity to tumor antigens. We show that the vaccination of BALB/c mice with BoHV-4 expressing xCT (BoHV-4-mxCT), impaired lung metastases induced by syngeneic mammary CSCs both in preventive and therapeutic settings. Vaccination induced T lymphocyte activation and the production of anti-xCT antibodies that can mediate antibody-dependent cell cytotoxicity (ADCC), and directly impair CSC phenotype, self-renewal and redox balance. Our findings pave the way for the potential future use of BoHV-4-based vector targeting xCT in metastatic breast cancer treatment.

ARTICLE HISTORY

Received 22 February 2018
Revised 22 June 2018
Accepted 24 June 2018

KEYWORDS

Mammary cancer;
cancer stem cell; xCT;
immunotherapy; bovine
herpesvirus 4-based vector

Introduction

Breast cancer is a deadly disease that affects millions of women worldwide. Despite advances in diagnosis and treatment, it is still the second cause of cancer death in women worldwide.¹ Local and distant tumor recurrence occurs in a high percentage of patients and metastases are the main cause of mortality.² Novel therapies to treat metastatic breast cancer therefore become a necessity.

Recurrence and metastatic disease in breast cancer and most solid tumors have been ascribed to a small cancer cell population with stem-like properties, referred to as cancer stem cells (CSCs).³ CSCs escape cell cycle regulation and cell death, are endowed with unlimited self-renewal potential and tumor-initiating capacity as well as expressing epithelial to mesenchymal transition (EMT) markers, which enable them to migrate and initiate metastases. Moreover, CSCs overexpress many detoxifying enzymes and possess increased drug efflux and DNA repair capacities, which render them resistant to radiotherapy and cytotoxic drugs.⁴ Much effort has therefore been dedicated to identify novel targets and therapies to specifically impact CSCs.⁵

We have identified the cystine-glutamate antiporter protein, xCT (SLC7A11), the light chain of the antiporter system x_c^- , as an oncoantigen (a tumor-associated antigen with a central role

in cancer development and progression⁶), that is overexpressed in human and mouse mammary CSCs.⁷ xCT plays an important role in maintaining intracellular redox balance, as it mediates the exchange of intracellular glutamate with extracellular cystine and thus promotes the synthesis of the anti-oxidant glutathione (GSH), thereby controlling intracellular reactive oxygen species (ROS) levels and chemosensitivity.⁸ Moreover, xCT expression creates a reducing extracellular microenvironment, in a GSH-independent manner, by promoting a redox cycle in which cystine is taken up by cells and reduced to cysteine, some of which is secreted via constitutively expressed neutral amino acid transport systems.⁹ Recent evidence shows that xCT also assists in protection from ferroptosis,⁸ and in cell metabolism regulation.¹⁰ xCT is only expressed by a few normal cell types (astrocytes, microglia and some myeloid cells),⁷ while it is overexpressed in numerous cancers, including a high percentage of mammary tumors.^{11–15} xCT expression has been observed in the CSCs of several cancer types, such as glioblastoma, colorectal, lung and gastric cancers,¹⁶ where it is stabilized on the cell membrane via interaction with two stem cell markers, Mucin-1 and CD44v.¹⁷ xCT is therefore a promising target for the treatment of many cancers. In fact, research has demonstrated that

CONTACT Federica Cavallo  federica.cavallo@unito.it  Department of Molecular Biotechnology and Health Sciences - Molecular Biotechnology Center, Università degli Studi di Torino, Via Nizza, 52 - 10126 - Torino, Italy; Laura Conti  laura.conti@unito.it  Department of Molecular Biotechnology and Health Sciences - Molecular Biotechnology Center, Università degli Studi di Torino, Via Nizza, 52 - 10126 - Torino, Italy

*These authors contributed equally.

Color versions of one or more of the figures in the article can be found online at www.tandfonline.com/koni.

 Supplemental data for this article can be accessed [here](#).

© 2018 Taylor & Francis Group, LLC

xCT down-modulation and inhibition exert antitumor effects by impairing tumor growth and metastatic dissemination in pre-clinical models.¹⁸ Moreover, preclinical experiments have shown that xCT disruption impairs the ROS defense system and sensitizes CSCs to chemotherapy, enhancing the therapeutic efficacy of doxorubicin, cisplatin and temozolomide.^{7,19,20} This evidence has led to xCT inhibitors, either used in combination with chemotherapy or alone, being investigated in a number of clinical trials on cancer patients. The most commonly used xCT inhibitor is sulfasalazine (SASP), an anti-inflammatory drug approved by the FDA and EMA for the treatment of inflammatory bowel disease, ulcerative colitis and Crohn's disease. However, SASP is poorly bioavailable, induces many side effects and is not xCT-specific, since it also inhibits NF- κ B *in vivo*.²¹ This may explain why clinical trials involving SASP administration have not produced the expected results.

Our search for new means to disrupt xCT functionality in CSCs has focused on active immunotherapy; anti-cancer vaccines are a promising strategy, as suggested by the advanced clinical testing that several have undergone in recent years.²²⁻²⁴ We have previously demonstrated that a DNA-based vaccine that expresses the full-length murine (m)xCT protein,⁷ and a virus-like particle, which displays the sixth extracellular loop of human xCT,²⁵ induce an anti-xCT humoral response in BALB/c mice that was able to impair murine and human mammary CSC self-renewal *in vitro* and hinder mammary tumor growth and lung metastases in syngeneic tumor models. We herein explore Bovine Herpes Virus-4 (BoHV-4) use as a viral vector to deliver the full length xCT DNA, as we have previously demonstrated it is superior to DNA vaccination in inducing an anti-HER2 antibody response in tolerant HER2 transgenic BALB-neuT mice.²⁶ Moreover, BoHV-4 vaccination has the potential to induce an immune response against various xCT epitopes as our DNA vaccine, but does not require electroporation, avoiding the use of anesthetics and concerns about patient compliance.

The immunization of mice with a BoHV-4 vector that expresses the full-length mxCT protein (BoHV-4-mxCT) induces T lymphocyte activation and the production of anti-xCT antibodies that can target CSCs both directly, by impairing self-renewal and increasing ROS content and ferroptosis, and via the induction of antibody-dependent cell cytotoxicity (ADCC). This immune response inhibited lung metastases that were either generated by the injection of CSCs derived from HER2/neu⁺ TUBO²⁷ or from triple negative 4T1 mammary cancer cells in syngeneic BALB/c mice in preventive and therapeutic settings, respectively.

Results

Generation of a recombinant virus that delivers mxCT expression cassette

An optimized open reading frame (ORF), coding for mxCT (Slc7a11), was customized by adding a 33 aa peptide tag, derived from bovine herpesvirus-1 glycoprotein D (gD₁₀₆),²⁸ (Supplementary Figure 1A), to its C-terminal to generate mxCTgD106 ORF. mxCTgD106 ORF was located downstream of the CMV promoter and upstream of the growth hormone polyadenylation signal to give the CMV-mxCTgD106 expression cassette, whose functionality was tested via western blotting with a

mAb to gD106. CMV-mxCTgD106 was excised from the plasmid backbone and sub-cloned into the pINT2 shuttle vector, which contained two BoHV-4 TK flanking sequences²⁹ (pTK-CMV-mxCTgD₁₀₆-TK), to generate pINT2-CMV-mxCTgD₁₀₆. This construct's protein expression was validated by transient transfection into HEK293T cells and immunoblotting (Supplementary Figure 2). A genomic molecular clone, obtained from a BoHV-4 that was isolated from the milk cell fraction of a clinically healthy cow (designated as BoHV-4-A),³⁰ was used to generate the BoHV-4-A-CMV-mxCTgD₁₀₆ recombinant virus; pINT2-CMV-mxCTgD₁₀₆ was linearized and electroporated into SW102 *E. coli* cells that contained the artificial chromosome pBAC-BoHV-4-A-KanaGalK Δ TK,^{30,31,32,33,34,35,36} (Figure 1A), and by heat-induced homologous recombination,³⁷ generated pBAC-BoHV-4-A-CMV-mxCTgD₁₀₆. The TK locus of the BoHV-4 genome was chosen for its extreme stability after repeated *in vitro* and *in vivo* passages, and because it is reliable when integrating foreign DNA sequences into the BoHV-4 genome without any transgene or viral replication efficiency loss due to recombination. Viral particles were generated from pBAC-BoHV-4-A-CMV-mxCTgD₁₀₆, and the replication properties of BoHV-4-mxCT were compared to those of the parental BoHV-4-A virus. The replication rate of BoHV-4-mxCT is slightly lower than in BoHV-4-A (Figure 1D). However, BoHV-4-mxCT-transduced cells expressed mxCT, as revealed by western blotting (Figure 1E). A virus expressing the unrelated A29 Monkeypoxvirus glycoprotein (BoHV-4-A29)³⁸ was used as a control.

BoHV-4-mxCT vaccination induces an anti-mxCT humoral response

Sera from BoHV-4-mxCT- and BoHV-4-A29-vaccinated mice were collected, as well as untreated mice sera, 2 weeks after the last vaccination, and tested by ELISA. Figure 2A shows that BoHV-4-mxCT induced an antibody response against the mxCT protein. The sera were tested in ELISA for their ability to bind the extracellular portions of xCT to better evaluate the therapeutic potential of these antibodies. Figure 2B-F demonstrates that BoHV-4-mxCT-induced antibodies recognized the extracellular domains of mouse xCT. Sera from BoHV-4-A29-vaccinated mice also bound, with a lower affinity, to full length mouse xCT and to its 6th extracellular loop (Figure 2A, F), which could be explained by the identity of 3 residues in A29 and xCT 6th extracellular loop, which is sufficient to induce cross-reactivity.³⁹ BoHV-4-mxCT induced antibodies also recognized xCT protein in its native conformation, as shown by the decoration of xCT⁺ tumorspheres by BoHV-4-mxCT-vaccinated mice sera (Figure 2G). Finally, this binding ability resulted in the activation of ADCC against xCT⁺ tumor cells, as demonstrated by incubating 4T1 target cells with the sera of BoHV-4-mxCT vaccinated mice in the presence of splenocytes from unvaccinated mice (Figure 2H).

BoHV-4-mxCT-induced antibodies target CSCs and impair mxCT function

To evaluate the direct effect exerted by BoHV-4-mxCT-induced antibodies on mammary CSCs, TUBO-derived tumorspheres were incubated for 5 days with sera from either control or

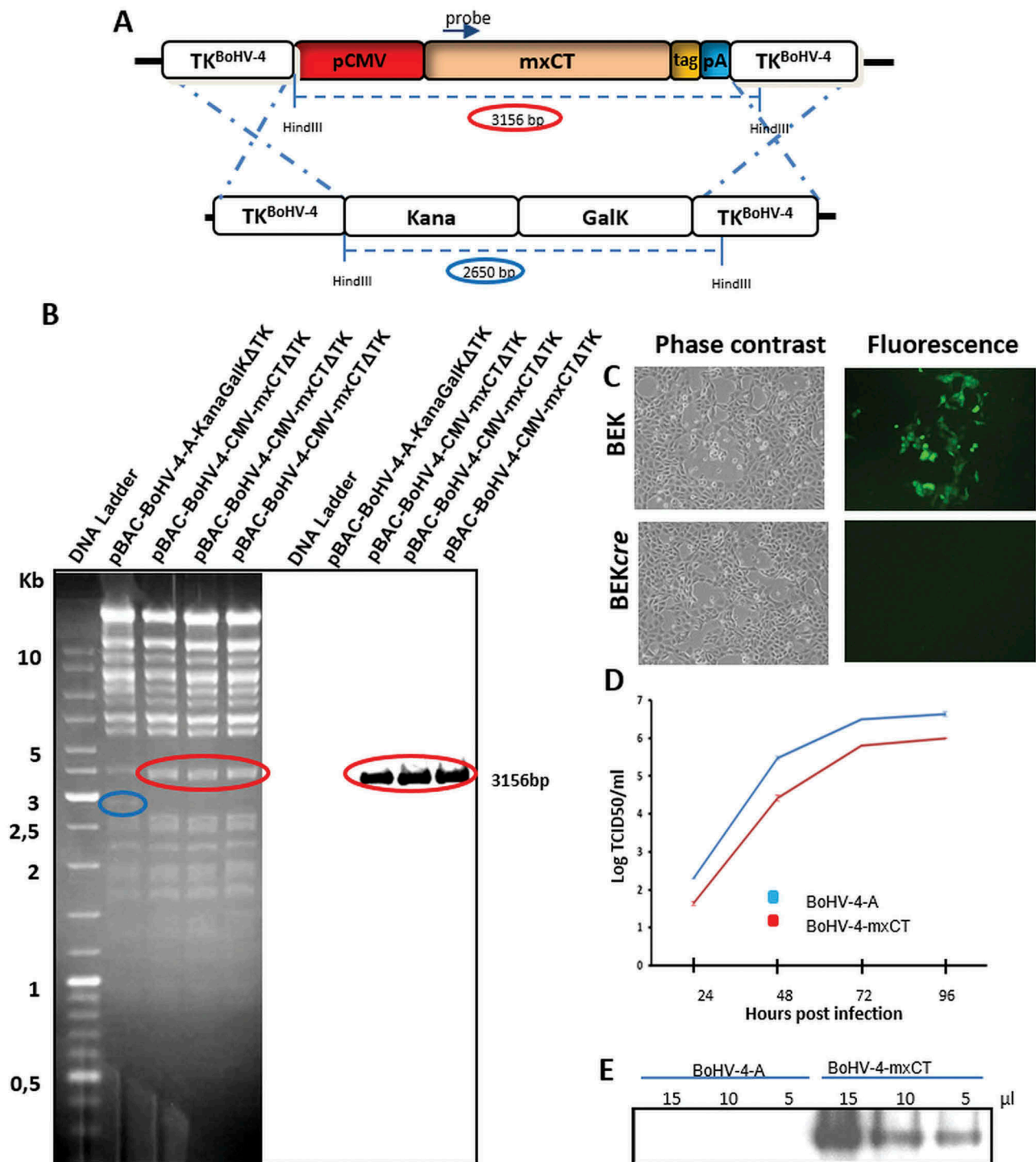


Figure 1. Generation of BoHV-4-mxCT. **A**) Diagram (not to scale) showing the retargeting event obtained by heat-inducible homologous recombination in SW102 *E. coli* containing pBAC-BoHV-4-A-TK-KanaGalK-TK, where the Kana/GalK cassette was replaced with the CMV-mxCTgD₁₀₆ expression cassette flanked by BoHV-4 TK sequences, located in pINT2 shuttle plasmid vector. **B**) Representative 2-deoxy-galactose resistant colonies tested by *HindIII* restriction enzyme analysis, agar gel electrophoresis and Southern blotting performed with a specific probe for the mxCT ORF. The 2,650 bp band (blue circle), corresponding to the un-retargeted pBAC-BoHV-4-A-TK-KanaGalK-TK control, has been replaced by a 3156 bp band (red circle) in pBAC-BoHV-4-A-CMV-mxCTgD₁₀₆ΔTK. **C**) Representative phase contrast and fluorescent microscopic images of plaque formed by viable reconstituted recombinant BoHV-4-mxCT after the corresponding BAC DNA electroporation into BEK cells expressing *cre* recombinase (Magnification, 10X). **D**) Replication kinetics of BoHV-4-mxCT growth on BEK cells compared with the parental BoHV-4-A isolate. The data presented are the means \pm SEM of triplicate measurements ($P > 0.05$ for all time points as measured by Student's *t*-test). **E**) Western immunoblotting of cells infected with BoHV-4-mxCT or the parental BoHV-4-A used as a negative control. The lanes were loaded with different amounts of total protein cell extracts (5, 10 and 15 μ l).

vaccinated mice, or with the xCT inhibitor SASP (control). Whereas sera from untreated or BoHV-4-A29 vaccinated mice did not induce tumorsphere alterations in terms of morphology, sphere number and dimension as compared with tumorspheres

grown in medium alone, sera from mice vaccinated with BoHV-4-mxCT induced a reduction in sphere number and dimension. Tumorsphere dimension was further decreased by SASP treatment, suggesting that it is very efficient in slowing tumorsphere

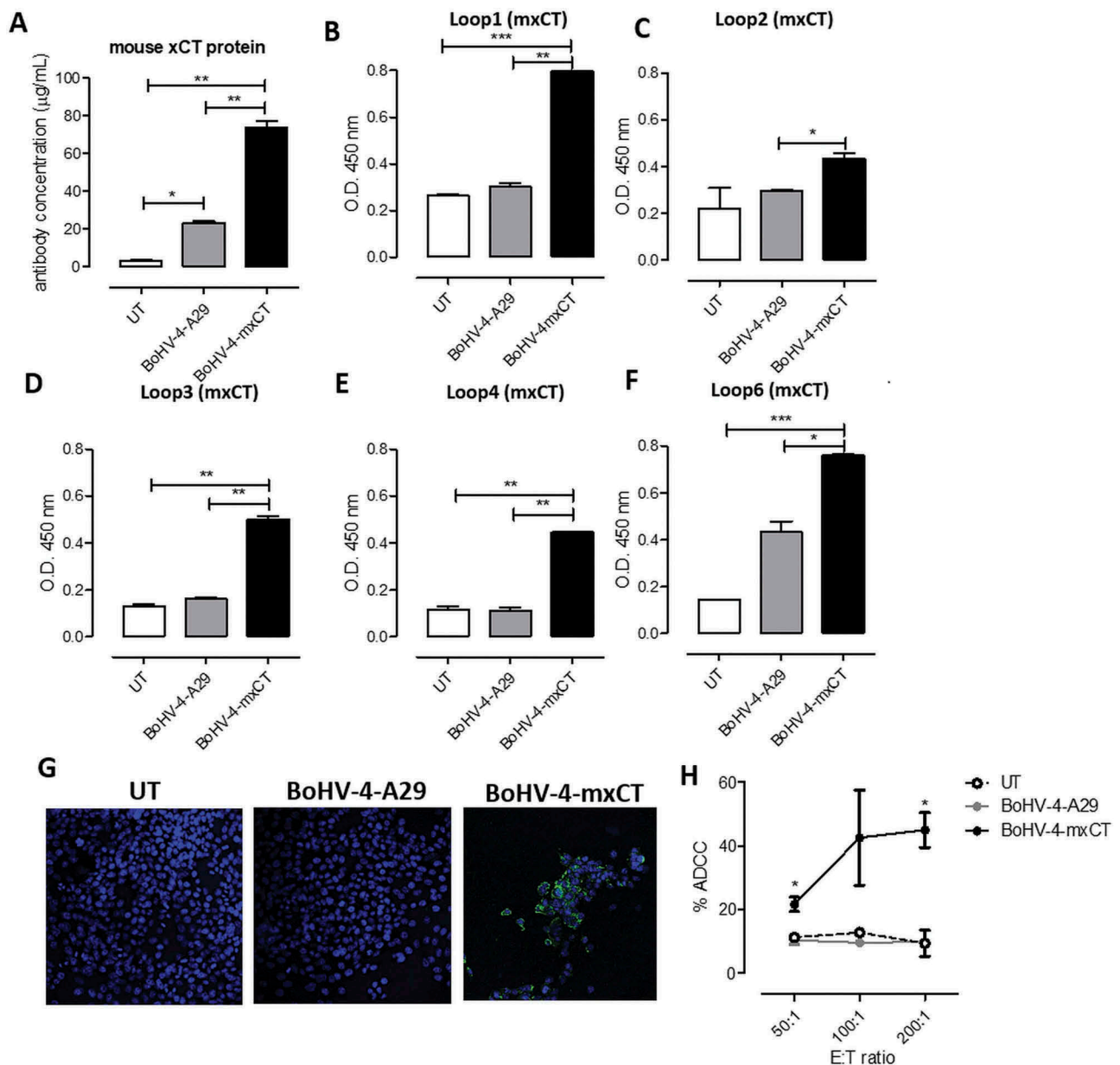


Figure 2. BoHV-4-mxCT vaccination induces an anti-xCT humoral response. Sera from untreated (white bars), BoHV4-A29- (gray bars) and BoHV-4-mxCT- (black bars) vaccinated mice were tested by ELISA on wells coated with **A**) full-length mouse xCT protein, or peptides corresponding to mouse xCT extracellular loops **B**) 1, **C**) 2, **D**) 3, **E**) 4 or **F**) 6. Graphs show mean \pm SEM of sera pooled from 3 independent experiments. In **A**, antibody concentration was calculated based on a standard curve obtained with a commercial anti-xCT antibody targeting its N-terminal region. **G**) Representative immunofluorescence images of dissociated 4T1 tumorsphere cells incubated with sera of vaccinated mice. The specific signal (green), was detected using an Alexa Fluor488-conjugated anti-mouse secondary antibody. Nuclei were counterstained with DAPI (blue). Magnification 40X, Scale bar, 40 μ m. **, $P < 0.01$, Student's *t*-test. **H**) ADCC assay performed using CFSE⁺ 4T1 target cells incubated with 1:50 pooled sera from untreated, BoHV-4-A29- and BoHV-4-mxCT-vaccinated mice and splenocytes from untreated mice as effector cells at different effector/target cells ratios (200:1, 100:1, and 50:1). Results shown are the mean \pm SEM of the percentage of ADCC, calculated as in Material and Methods.

growth (Figure 3A-C). BoHV-4-mxCT and SASP effects on tumorsphere generation were accompanied by a slight inhibition in cell cycle progression, as demonstrated by the increase in quiescent cells in the G0/G1 phase, when compared with control cells (Figure 3D). BoHV-4-mxCT sera and SASP seemed to be able to target CSCs as they lowered the percentage of cells positive for the Aldefluor reagent, a non-immunological method to identify CSCs on the basis of their aldehyde dehydrogenase-1 (ALDH) activity (Figure 3E, F). Indeed, high ALDH expression is considered a marker of CSCs of various lineages, including breast cancer.⁴⁰ Moreover, both SASP and, to a greater extent, sera from BoHV-4-mxCT-treated mice altered CSC redox

balance, inducing an intracellular ROS accumulation (Figure 3G, H). The ROS content increase in cells treated with BoHV-4-mxCT-vaccinated mice sera or SASP was accompanied by an increase in Chac1 glutathione-specific gamma-glutamylcystotransferase 1 (Chac1) mRNA content (Figure 3I), which is significantly elevated in cells undergoing endoplasmic reticulum stress and ferroptosis.⁸ Interestingly, BoHV-4-mxCT-vaccinated mice sera and, to a greater extent, SASP, also upregulated xCT mRNA (Figure 3L).

Overall, these results indicate that BoHV-4-mxCT vaccination induces the production of antibodies that alter CSC self-renewal and redox balance. These results were not confined to

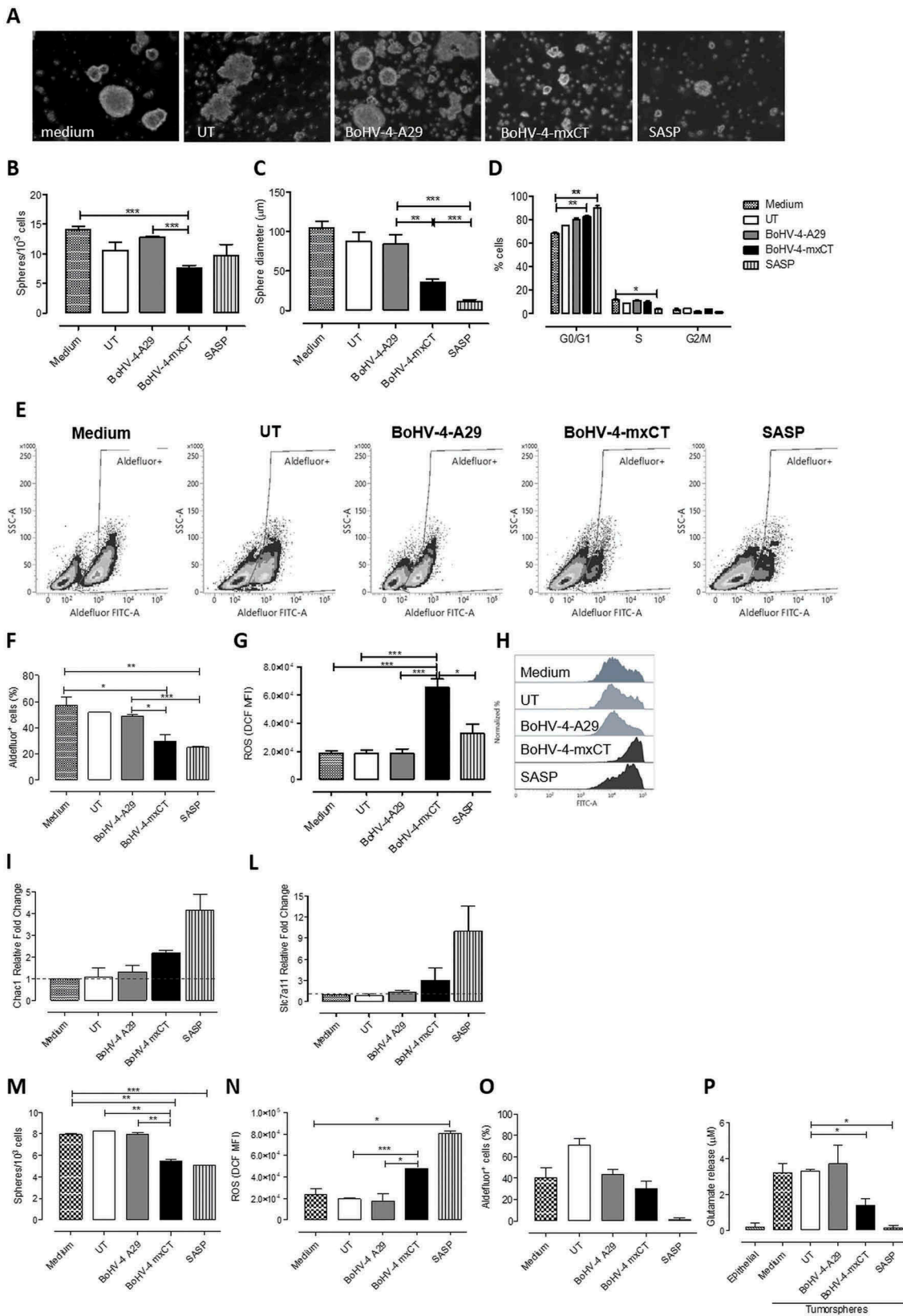


Figure 3. BoHV-4-mxCT induces antibodies to target CSCs and affects self-renewal and ROS flux. TUBO A-L)– and 4T1 M-P)–derived tumorspheres were incubated for 5 days with medium, sera of untreated, BoHV-4-A29- and BoHV-4-mxCT-vaccinated mice, or with SASP (50 μM). **A)** Representative images of tumorspheres, magnification 40X, scale bar 40 μm . **B)** Sphere generating ability reported as tumorsphere number/ 10^3 plated cells. **C)** Sphere diameter measured with the AxioVision 4.8 software. **D)** Percentage of cells in the different phases of the cell cycle, as measured by FACS analysis using propidium iodide **E-F)** Aldefluor positivity reported as percentage of positive cells or as representative density plots. **G-H)** FACS analysis of ROS production, reported as DCF MFI or shown as representative histograms. **I-L)** Real time PCR of the ferroptosis marker Chac1 or of xCT. All graphs show mean \pm SEM from at least three independent experiments. **M)** Sphere generating ability reported as tumorsphere number/ 10^3 plated cells. **N)** FACS analysis of ROS production, reported as DCF MFI. **O)** Aldefluor positivity reported as percentage of positive cells. **P)** Evaluation of glutamate in the supernatants of treated 4T1 tumorspheres or of parental 4T1 cells cultured as monolayers. *, $P < 0.05$; **, $P < 0.01$, ***, $P < 0.001$, Student's t -test.

the TUBO model, since sera from BoHV-4-mxCT-vaccinated mice also reduced tumorsphere self-renewal, increased ROS content and decreased Aldefluor⁺ CSC number in 4T1 cells (Figure 3M-O). Moreover, BoHV-4-mxCT-induced antibodies and, to a greater extent, SASP significantly inhibited glutamate export by 4T1 tumorspheres, reducing the amount of glutamate in the supernatant of treated tumorspheres to levels similar to those in epithelial 4T1 parental cells (Figure 3P).

Interestingly, BoHV-4-mxCT-induced antibodies cross-reacted with human xCT, decreased CSC self-renewal and increased ROS content in human HER2⁺ SKBR3 breast cancer cells (Supplementary Figure 3).

Vaccination with BoHV-4-mxCT prevents TUBO lung metastases

To test the BoHV-4-mxCT-induced immune response's ability to prevent mammary CSC seeding in lungs, BALB/c mice were vaccinated twice, at two-week intervals, with BoHV-4-mxCT, or BoHV-4-A29 or left untreated (negative controls). After 7 days, mice were injected intravenously (i.v.) with syngeneic CSC-enriched,²⁷ xCT⁺ TUBO tumorsphere-derived cells,⁷ and lung metastasis number was evaluated three weeks later. Whereas lungs from untreated and BoHV-4-A29-vaccinated mice showed a high number of macrometastases, lungs from BoHV-4-mxCT-vaccinated mice only displayed isolated macrometastases, as shown in Figure 4A. These results were confirmed in a micrometastases analysis in H&E-stained lung sections (Figure 4B), in which BoHV-4-mxCT-vaccinated mice showed a significant decrease in the percentage of lung tissue occupied by metastases (Figure 4C), and in the number of metastases per square mm (Figure 4D), relative to control mice. Overall, these data indicate that BoHV-4-mediated xCT immunotargeting prevents mammary CSC seeding in the lungs.

Vaccination with bohv-4-mxct reduces mammary cancer growth and metastatic dissemination in a therapeutic setting

To investigate the ability of therapeutic vaccination to reduce tumor growth and spontaneous lung metastatization in mice with existing tumors, 4T1 tumorsphere-derived cells were transplanted subcutaneously (s.c.) into mice. When s.c. tumors reached 2 mm mean diameter, mice were vaccinated twice, at two-week intervals. Tumor growth rate, measured as tumor volume progression over time, was significantly lower in the BoHV-4-mxCT-vaccinated group than in the untreated and BoHV-4-A29-vaccinated groups (Figure 4E). Mice were culled, lungs harvested and subsequently histologically analyzed twenty days after tumor cell challenge. BoHV-4-mxCT significantly reduced the percentage of metastatic area and spontaneous micrometastasis number in the lungs (Figure 4F-H), suggesting that vaccination with BoHV-4-mxCT may be a new approach to mammary cancer treatment.

BoHV-4-mxCT induces T lymphocyte activation in the lungs of vaccinated mice

To further characterize the immune mechanisms that mediate BoHV-4-mxCT anti-metastatic potential, the immune cell

infiltrate in the lungs of vaccinated mice was analyzed three weeks after TUBO-derived tumorsphere i.v. injection. CD11b⁺ Ly6G⁺ neutrophils and granulocytic myeloid-derived suppressor cells (gMDSC) were the predominant myeloid cell population in metastatic lungs, while CD11b⁺Ly6C⁺ monocytic myeloid-derived suppressor cells (mMDSC), CD11b⁺ F4/80⁺ macrophages and CD11c⁺ dendritic cells only represented a minority. However, no significant differences in myeloid cell population proportions were observed in the treatment groups (Figure 5A). The percentages of T lymphocytes (CD3⁺) and Natural Killer (NK, CD3⁻CD49b⁺) cells among the CD45⁺ leucocytes did not vary significantly (Figure 5B, G), and most T cells were CD4⁺. No significant CD4⁺/CD8⁺ T cell ratio alterations were detected, although both BoHV-4-A29 and BoHV-4-mxCT slightly increased the CD8⁺ cell percentage in the CD3⁺ T cell population (Figure 5C). Interestingly, BoHV-4-mxCT vaccination induced T cell activation, as suggested by the significant increase in CD69⁺ cells in the total CD3⁺ T cell population (Figure 5D), and in both CD4⁺ T helper, and CD8⁺ T cytotoxic cells (Figure 5D, H). Moreover, BoHV-4-mxCT significantly increased the expression of immune checkpoint and exhaustion marker molecule PD1 in CD4⁺, CD8⁺ T and NK cells (Figure 5E, H). These data suggest that BoHV-4-mxCT vaccination may benefit from association with anti-PD1 and/or anti-PD-L1 monoclonal antibody therapy. In fact, PD-L1 was expressed by a small percentage of epithelial and myeloid cells in the lungs, and BoHV-4-A29 and BoHV-4-mxCT vaccination slightly increased its expression in epithelial cells (Figure 5F).

BoHV-4-mxCT vaccination induces the generation and expansion of effector T lymphocytes

To further characterize the T cell response induced by BoHV-4-mxCT vaccination, spleens from vaccinated mice that did not receive tumor cell injection were harvested and T cells were evaluated for their response against xCT. When splenocytes were re-stimulated with 15 µg/ml of H-2K^d dominant mouse xCT (S Y A E L G T S I) peptide⁷, no specific IFN-γ production was detected by ELISPOT (data not shown), suggesting that high-avidity CD8⁺ T-cell clones could have been depleted during thymic selection, as we have previously reported for the HER2 antigen in the BALB-neuT model⁴¹. However, when splenocytes were cultured overnight with Mitomycin C-treated xCT⁺ 4T1 cells, an increase in the percentage of CD4⁺ T cells expressing the CD69 activation marker was observed in BoHV-4-mxCT splenocytes (Figure 6A), accompanied by a statistically significant increase in IFN-γ-producing helper T cells and a trend of increase in CD107⁺ cytotoxic CD4⁺ T cells (Figure 6B, C). Activation and IFN-γ production were higher in CD8⁺ T cells from BoHV-4-mxCT vaccinated mice than in the untreated mice (Figure 6D-F). The increased activation and IFN-γ production of both CD4⁺ and CD8⁺ T cells was maintained after 5 days of co-culture with 4T1 cells, when a statistically significant increase in CD107⁺ cytotoxic cells was also observed (Figure 6G-N). To test the ability of these activated T cells to induce cytotoxicity in 4T1 cells, an *in vitro* killing assay was performed by co-culturing effector splenocytes from control, BoHV-4-mxCT and BoHV-4-A29 vaccinated mice with CFSE-labeled 4T1

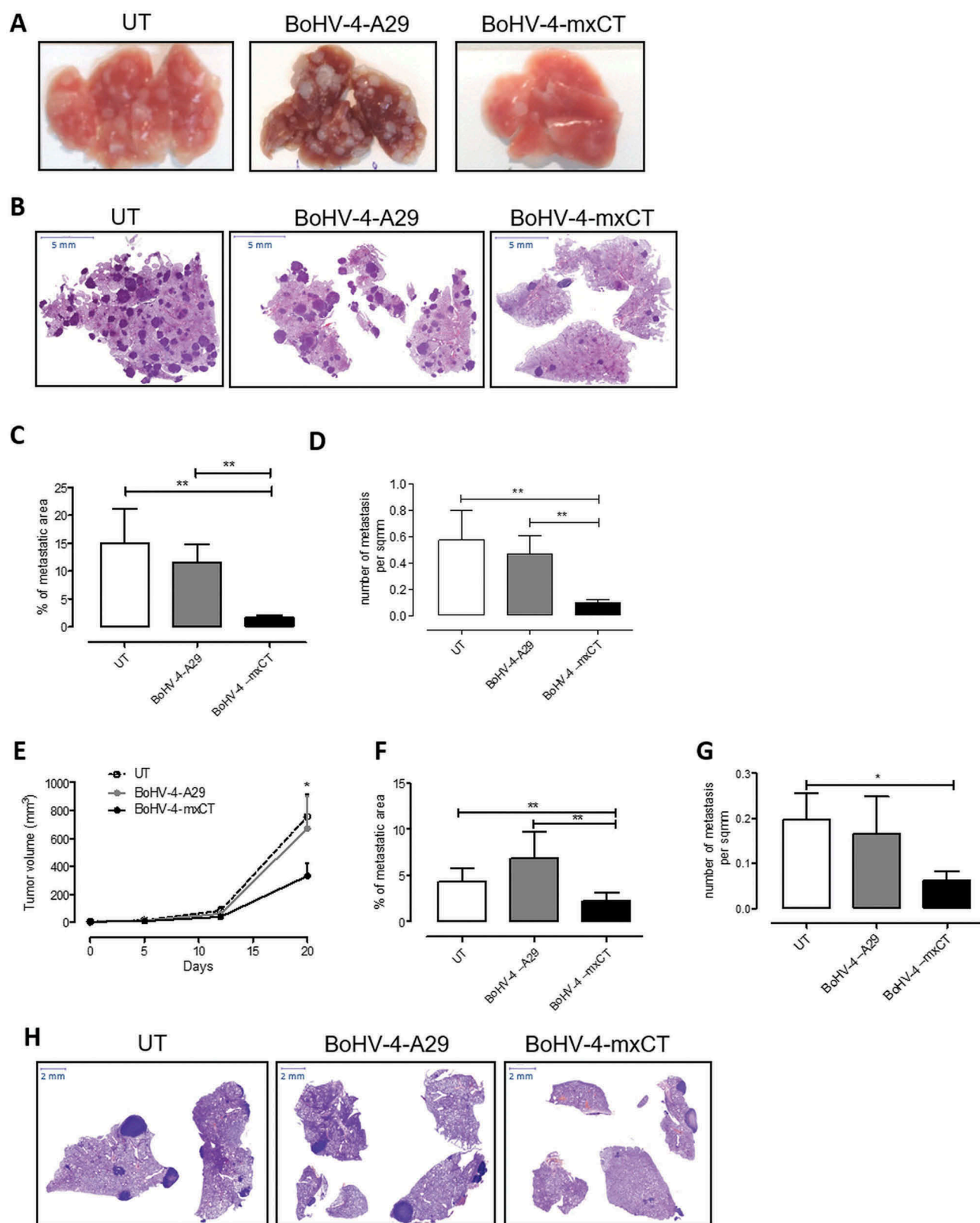


Figure 4. Vaccination with BoHV-4-mxCT decreases mammary cancer lung metastases. **A-D)** BALB/c mice were vaccinated twice with BoHV-4-mxCT, BoHV-4-A29 or left untreated. One week after the final administration, TUBO-derived tumorspheres were injected into the tail vein of treated mice. 20 days after cell challenge, lungs were removed, sectioned and micrometastasis number was determined in at least 2 H&E sections per mouse. **A)** Photograph of representative lungs, **B)** Representative images of lung metastases after H&E staining. Graphs showing **C)** the % of metastatic area and **D)** metastases number per square mm (sqmm), measured in mouse lungs from 3 independent experiments. **E-H)** BALB/c mice were s.c. challenged with 1×10^4 4T1 tumorsphere-derived cells. When the tumors reached 24 mm diameter, mice were vaccinated and boosted 14 days later. **E)** Subcutaneous tumor diameters were measured at the indicated time points and tumor volume was calculated. Graphs showing **F)** the % of metastatic area and **G)** the number of metastases per square mm measured in lungs. **H)** Representative images of lung metastases after H&E staining. * $P < 0.05$, ** $P < 0.01$, Student's *t*-test.

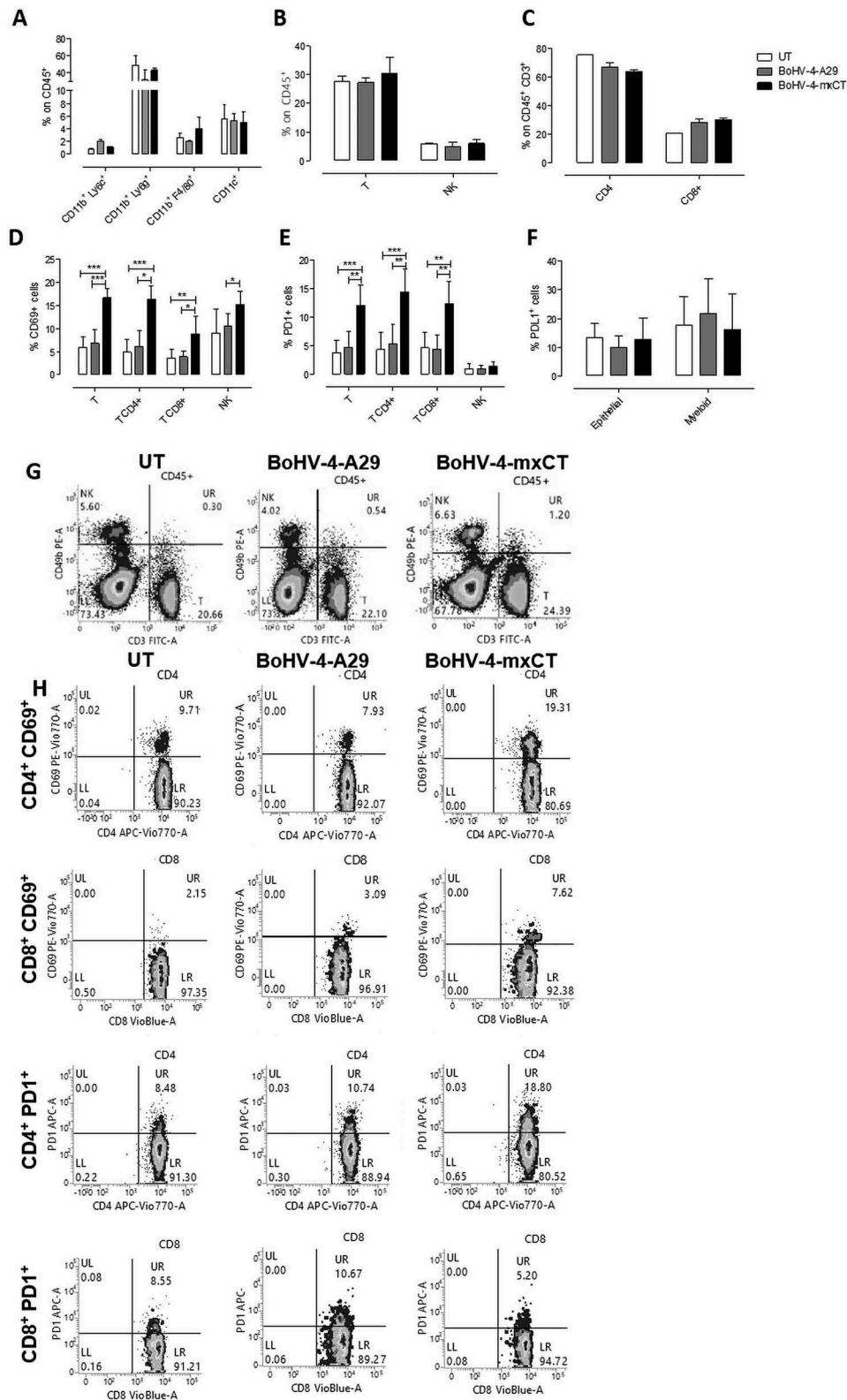


Figure 5. BoHV-4-mxCT induces lung T lymphocyte activation in vaccinated mice. Cytofluorimetric analysis of lung immune infiltrates in untreated (white bars), BoHV4-A29- (gray bars) and BoHV-4-mxCT- (black bars) vaccinated mice. **A)** Graph shows the percentage \pm SEM of CD45⁺ myeloid cells expressing the markers of mMDSC (CD11b⁺Ly6C⁺), neutrophil/gMDSC (CD11b⁺Ly6G⁺), macrophage (CD11b⁺F4/80⁺), and dendritic cell (CD11b⁺CD11c⁺) populations. **B)** Graph shows the percentage \pm SEM of CD45⁺ cells expressing the markers of T (CD3⁺CD49b⁺), and NK (CD3⁺CD49b⁺) populations. **C)** Percentage \pm SEM of CD4⁺ or CD8⁺ cells among the CD45⁺CD3⁺ T cell population. **D)** Percentage \pm SEM of CD69⁺ cells among total T, CD4⁺ or CD8⁺ T, and NK cell populations. **E)** Percentage \pm SEM of PD1⁺ cells among total T, CD4⁺ or CD8⁺ T, and NK cell populations. **F)** Percentage \pm SEM of PDL1⁺ cells among epithelial (CD45⁻) or myeloid (CD11b⁺) cells. **G-H)** Representative density plots showing **G)** CD3 and CD49b expression on CD45⁺ cells, and **H)** CD69 and PD1 expression on CD4⁺ or CD8⁺ T lymphocytes. *, P < 0.05; **, P < 0.01, ***, P < 0.001, Student's *t*-test.

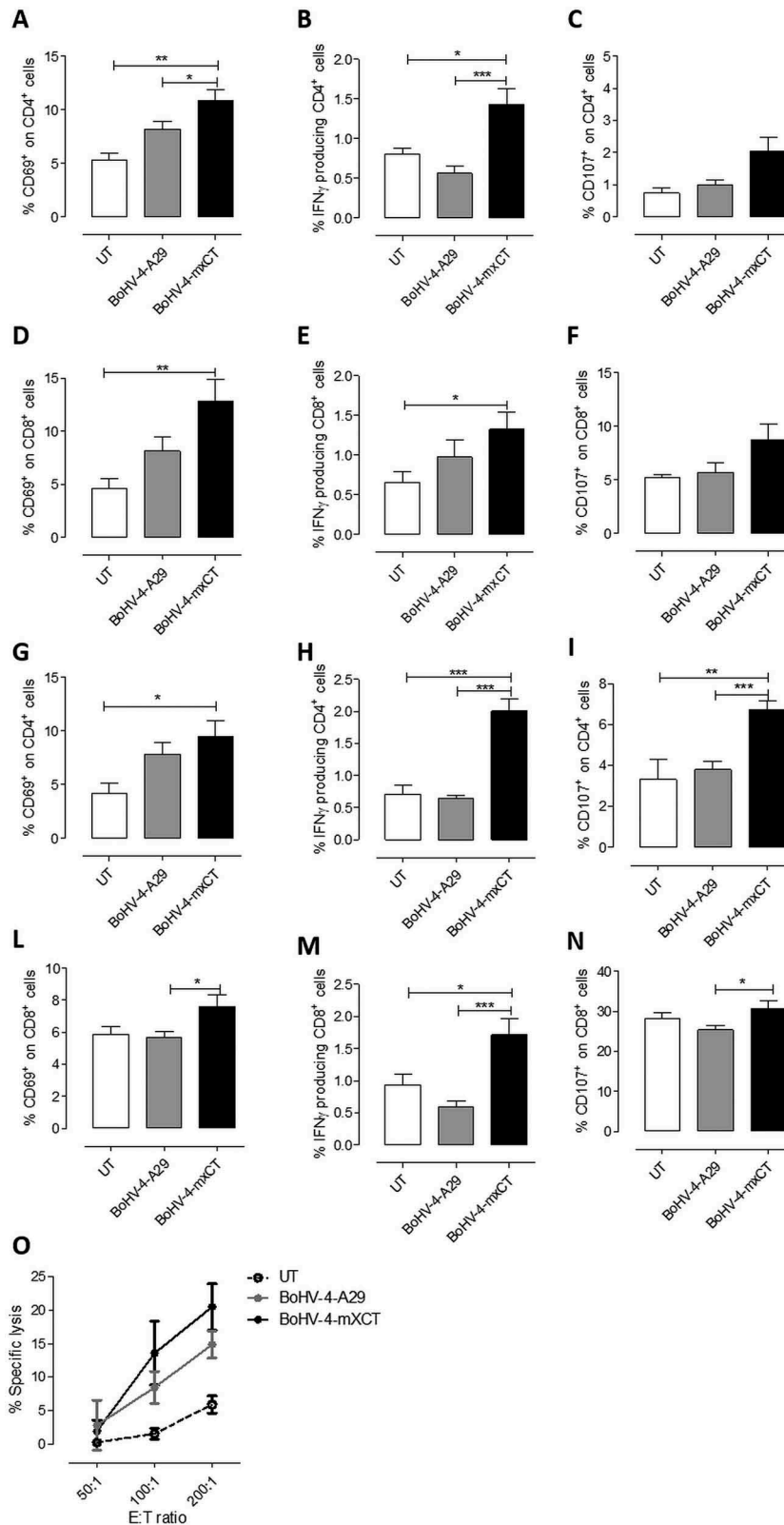


Figure 6. BoHV-4-mxCT vaccination induces degranulation and IFN- γ production in T lymphocytes. **A-N)** Splenocytes from untreated (white bars), BoHV4-A29- (gray bars), and BoHV-4-mxCT- (black bars), vaccinated mice, were co-cultured with mitomycin C treated 4T1 cells overnight (**A-F**) or for 5 days (**G-N**), incubated with FITC-conjugated antibodies against CD107a and b in the presence of Brefeldin A for 4 hours, then stained with antibodies against CD45, CD4, CD8, and CD69 and for intracellular IFN- γ and analyzed by FACS. Graphs show means \pm SEM of the percentages of **A-C, G-I**) CD4⁺ or **D-F, L-N**) CD8⁺ cells expressing **A, D, G, L**) CD69, **B, E, H, M**) IFN- γ or **C, F, I, N**) CD107 from three experiments. **O)** Splenocytes from untreated, BoHV4-A29 and BoHV-4-mxCT-vaccinated mice were co-cultured with CFSE⁺ 4T1 cells for 48 hours, then the percentage of 7-AAD⁺ dead cells among the CFSE⁺ target populations was analyzed by FACS. Graphs shows mean \pm SEM of the percentages of specific lysis, calculated as described in Material and Methods. *, $P < 0.05$; **, $P < 0.01$, ***, $P < 0.001$, Student's t -test.

target cells for 48 hours. BoHV-4-A29 and BoHV-4-mxCT splenocytes displayed enhanced lytic activity compared to untreated-mice splenocytes, but only a mild increase in BoHV-4-mxCT splenocyte cytotoxic activity over that of BoHV-4-A29 was observed (Figure 6O).

To evaluate *in vivo* the role of this vaccine-induced T cell response, vaccinated and control mice were depleted of CD4⁺ and CD8⁺ T cells, starting at the time of TUBO tumorsphere i.v. injection (Figure 7). While no significant differences in the percentage of metastatic area (Figure 7A) and the number of lung metastases (Figure 7B) were found in untreated and BoHV-4-A29 vaccinated mice following depletion, a significant increase in both parameters was observed in CD8-depleted mice vaccinated with BoHV-4-mxCT (Figure 7A, B). A significant increase in the percentage of metastatic area was also found in CD4-depleted BoHV-4-mxCT-vaccinated mice as compared to not-depleted vaccinated mice (Figure 7A). Since we have previously shown that CSC-enriched TUBO tumorspheres downregulated MHC class I expression,⁴² we hypothesized that BoHV-4-mxCT-induced antibodies could induce their differentiation and subsequent MHC class I expression. To confirm this hypothesis, TUBO tumorspheres were cultured for 5 days in the presence of sera from untreated, BoHV-4-A29 or BoHV-4-mxCT-vaccinated mice or with IgG purified from the sera of BoHV-4-mxCT-vaccinated mice. As shown in Figure 7C, both purified IgG and sera from BoHV-4-mxCT-vaccinated mice induced a significant increase in MHC class I expression as compared to the control conditions. However, MHC class I

upregulation induced by BoHV-4-mxCT sera was significantly higher than that induced by purified IgG, suggesting that the effect of anti-xCT IgG is amplified by the presence of vaccination-induced cytokines. Sera from BoHV-4-mxCT vaccinated mice induced also a mild increase in MHC class II and Fas expression (Figure 7C). It is thus conceivable that CD4⁺ and, to a greater extent, CD8⁺ cytotoxic T cells contribute to the anti-metastatic effects of BoHV-4-mxCT vaccination.

Discussion

The recent clinical successes of checkpoint blocking antibodies and the discovery of cancer neoantigens have renewed interest in immunotherapy, which is entering a golden age. However, therapeutic cancer vaccines have not yet provided the expected clinical results, which would intensify the search for better tumor antigens and vaccine formulations. Moreover, the discovery that CSCs are the main source of tumor recurrence highlights how developing vaccines towards CSC-expressed antigens may treat metastatic cancer. We have previously shown that xCT is overexpressed in breast CSCs, where it plays a key role in the maintenance of self-renewal and redox balance,⁷ making it a potential CSC oncoantigen. In physiological conditions, xCT expression is confined to specialized areas in the brain, spleen and thymus,⁴³ while its expression is enhanced on tumor cells in pancreatic, gastrointestinal, glioblastoma and colorectal cancers.⁷ Indeed, xCT provides increased antioxidant capability allowing cancer cells to grow and resist to chemo- and radiotherapy.²⁰ Therefore, in several cancers,

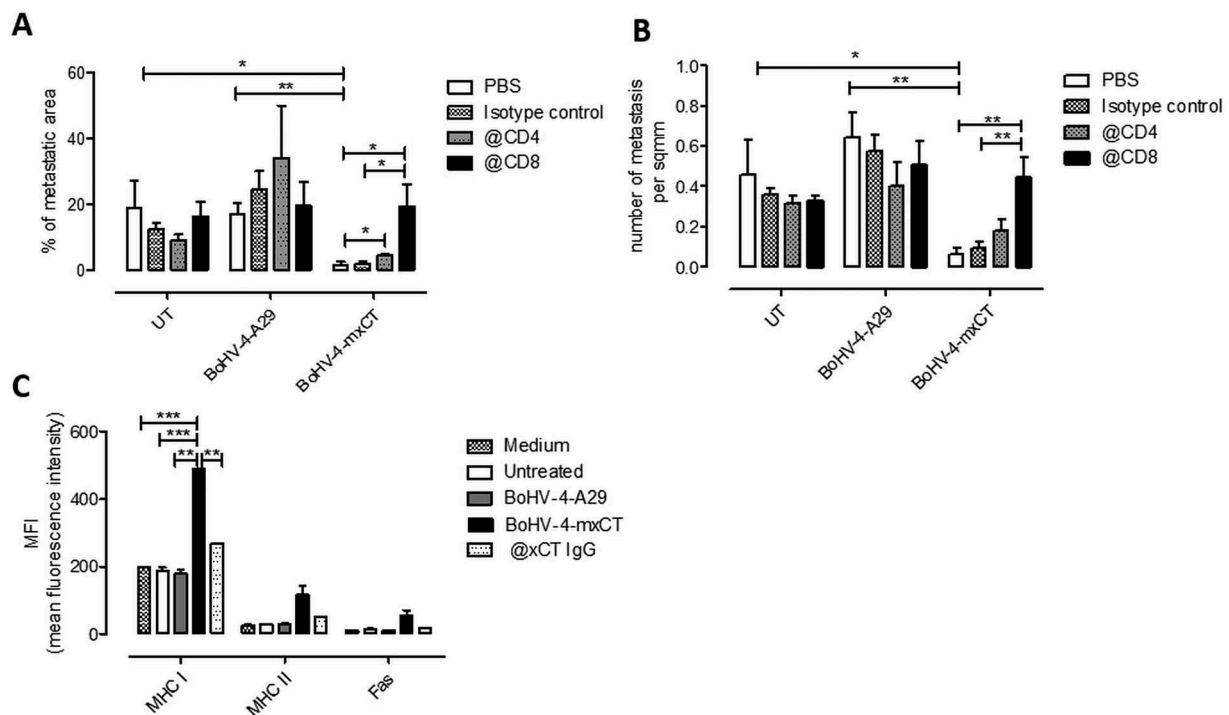


Figure 7. Depletion of T lymphocytes impairs BoHV-4-mxCT anti-metastatic activity. A, B) BALB/c mice were vaccinated twice with BoHV-4-mxCT, BoHV-4-A29 or left untreated. One week after the final vaccination, TUBO-derived tumorspheres were injected intravenously. Mice were then treated i.p., every 3 days, with either PBS or 200 μ g of anti-CD4 (@CD4), anti-CD8 (@CD8) or isotype control antibodies. 20 days after cell challenge, lungs were removed, sectioned and micrometastasis number was determined in H&E sections. Graphs showing means \pm SEM of A) the % of metastatic area and B) metastasis number per square mm (sq mm) ($n = 5$ per group). C) TUBO-derived tumorspheres were incubated for 5 days with medium, sera of untreated, BoHV-4-A29- or BoHV-4-mxCT-vaccinated BALB/c mice, or with IgG purified from sera from BoHV-4-mxCT-vaccinated mice (50 μ g/ml@xCT). FACS analysis of MHC class I, MHC class II and Fas, reported as means \pm SEM of MFI from three experiments. *, $P < 0.05$; **, $P < 0.01$, ***, $P < 0.001$, Student's *t*-test.

increased xCT expression is predictive for poor survival,¹¹ making its immune-targeting of great clinical interest.

We have previously demonstrated that xCT immune-targeting, by means of VLPs or DNA vaccination, induced a specific humoral response that hampered breast cancer growth and metastasis in preclinical models of triple negative and HER2⁺ breast cancers. However, these immunotherapies did not induce specific T cell activation, since xCT is a self-tolerated antigen and thymic depletion of high-avidity T-cell clones can occur.^{7,25}

This work has focused on viral-vectors as a means to breaking tolerance and inducing a strong immune response, and has developed a BoHV-4-based vaccine that targets xCT. We have previously demonstrated that BoHV-4 can be used to express exogenous antigens in various cell types in several animal species without pathogenicity or oncogenicity.^{32,44} Moreover, when engineered to express HER2-derived antigens, it can protect HER2 transgenic BALB-neuT mice from autochthonous mammary cancer.²⁶

A mouse xCT-expressing BoHV-4 vector was thus generated to inhibit the seeding of HER2⁺ CSCs to the lungs in BALB/c mice, preventing the formation of pulmonary metastases. Of greater clinical interest is BoHV-4-mxCT's ability to decrease the cancer growth, spontaneous metastatic spreading and lung metastasis formation induced by TNBC CSCs in a therapeutic setting, suggesting that it may benefit the 30% of TNBC patients who display xCT expression.¹¹

Cancer metastasis formation is a complex, multistage event involving continuous and finely tuned interplay between the microenvironment and cancer cells, while immune cell composition in the target organ is key in metastatic cell seeding.^{6,45} BoHV-4-mxCT vaccination induced activated T lymphocyte recruitment in metastatic lungs, and increased the percentage of CD4⁺ and CD8⁺ T cells that secreted IFN- γ in response to re-stimulation with xCT⁺ tumor cells. This is noteworthy because T lymphocyte infiltration is associated with good prognosis in breast cancer patients, while the activation of IFN- γ -producing T helper 1 and CD8⁺ T cells is important for anti-cancer response.⁴⁶ The re-stimulation of splenocytes from BoHV-4-mxCT-vaccinated mice with 4T1 cells also increased the percentage of CD107⁺ T cells. Nevertheless, only a very slight increase in the ability of splenocytes to kill 4T1 cells *in vitro* was detected when compared with splenocytes from BoHV-4-A29 control mice. Since CSCs down regulate MHC class I expression as an immune evasion mechanism,⁴² CD8⁺ cytotoxic T lymphocytes are only expected to play a marginal role in the immune surveillance of CSC metastatic spreading. This was confirmed by the absence of any effect of CD8 depletion in untreated and BoHV-4-A29 vaccinated mice. A different situation is found after BoHV-4-mxCT vaccination. Indeed, the induction of a T helper 1 response by BoHV-4-mxCT was accompanied by a specific humoral response, including polyclonal antibodies that can recognize xCT extracellular loops and bind CSC-enriched tumorspheres. These anti-xCT antibodies exert therapeutic activity through different mechanisms, one of which is induction of CSC differentiation and MHC class I expression, which makes them sensitive to CD8⁺ T cell killing. Indeed, depletion of CD8⁺ T cells in BoHV-4-mxCT vaccinated mice resulted in an increased development of lung metastases after an i.v. challenge of TUBO tumorspheres. The T helper 1 response potentiates this

effect through the release of IFN- γ that induces MHC class I expression. Moreover, this cytokine has been shown to induce MHC class II expression in cancer cells in TNBC and other tumors with a T cell infiltrate.⁴⁶ Indeed, in our model the sera from BoHV-4-mxCT-vaccinated mice led to upregulation of MHC class II expression in TUBO tumorspheres, and CD4⁺ cells depletion during the effector phase of vaccine-induced immune response slightly increased metastasis growth. This suggests the participation to immune response of CD4⁺ cytotoxic T lymphocytes, a cell population recently shown to lyse infected and neoplastic cancer cells in an MHC class II dependent manner.⁴⁷

Vaccine-induced anti-xCT antibodies participate in tumor cell elimination by activating the innate immune response via ADCC induction. Moreover, they can directly impair CSC self-renewal and arrest their cell cycle in the G1 phase. BoHV-4-mxCT-induced antibodies alter CSC redox balance by targeting xCT, which consequently increases intracellular ROS levels. Elevated ROS levels hamper CSC survival by decreasing β -catenin activation and consequently down-regulating stem cell genes, causing enhanced sensitivity to T cell cytotoxicity, as discussed above, chemo- and radiotherapy, and ferroptosis; a recently discovered form of cell death caused by ROS and iron-dependent lipid peroxide accumulation.⁴⁸ Indeed, elevated levels of the endoplasmic reticulum stress and ferroptosis marker Chac1⁸ were observed in CSCs treated with sera from BoHV-4-mxCT-vaccinated mice, confirming that this mechanism may contribute to BoHV-4-mxCT anti-metastatic effect.

Moreover, as xCT mediates glutamate export in exchange with cystine, BoHV-4-mxCT-induced antibodies lower extracellular glutamate levels. This makes the BoHV-4-mxCT vaccine an interesting tool for the treatment of patients with bone metastasis, a common characteristic of advanced breast cancer, since it has been demonstrated that glutamate released by cancer cells can disrupt normal bone turnover, favoring metastasis formation and possibly causing cancer-induced bone pain.⁴⁹ Moreover, high levels of extracellular glutamate have recently been shown to drive invasion through a paracrine signaling mediated by metabotropic glutamate receptors expressed in breast cancer cells.⁵⁰

Although xCT is a self-antigen, no overt adverse effects were observed in mice vaccinated with BoHV-4-mxCT, probably because its physiological expression is restricted to a few central nervous system and myeloid compartment cell types.^{7,51} The feasibility of xCT targeting in patients is supported by the extended usage of its inhibitor SASP in the clinical practice, for the treatment of many inflammatory diseases, without serious adverse events. Moreover, the safety of xCT immune targeting is further supported by the lack of immune infiltrate and abnormalities in the brains of mice vaccinated with VLPs that present xCT extracellular loops,²⁵ and by the fact that xCT knockout mice display normal development and no organ alterations.⁵²

A comparison of the immune responses induced by BoHV-4-mxCT and by the DNA- and VLP-based vaccines we have previously used to target xCT requires additional experiments. However, from the data already available, it is clear that in all cases the main effector mechanism is

represented by a T helper 1 immune response that results in anti-xCT IgG production.^{7,25} The highest specific antibody titer evaluated by ELISA was obtained with VLP vaccines, whose limitation – or advantage – is represented by the relatively small dimension of the xCT derived peptides they can display.⁵³ Instead, both DNA and BoHV-4 vaccines were designed to express the full length xCT protein, allowing the production of antibodies directed against different portions of xCT.⁵³ Moreover, while no specific T cell responses were detected in DNA and VLP vaccinated mice (even if no *in vivo* depletion experiments were performed),^{7,25} BoHV-4-mxCT induced a CD8 cytotoxic response, with a key role *in vivo*. This suggests that active immunization can be more effective than the passive administration of anti-xCT antibodies. Finally, despite inducing not completely identical immune responses, the anti-tumor and anti-metastatic efficacy of the three vaccines is very similar.^{7,25} This observation suggests that xCT immunotargeting, independently on the vector used, slows tumor growth and decreases metastasis formation but is not able to completely eradicate the disease. Therefore, anti-xCT vaccination should be combined with other anti-cancer strategies. Indeed, it has become ever clearer that combination therapies provide better patient survival results than single agents. xCT immune-targeting may be used as an add-on therapy together with conventional and innovative treatments that can further stimulate immune responses targeting differentiated cancer cells/CSCs. Combinations with anti-PD1 or PD-L1 monoclonal antibodies may improve therapeutic efficacy as BoHV-4-mxCT enhances activation and consequently PD1 expression on infiltrating T lymphocytes and we showed that PD-L1 is expressed on both CSCs and myeloid cells. The administration of anti-PD1 and anti-PD-L1 antibodies to breast cancer patients is currently undergoing clinical trial, and preliminary data show clinical activity in some TNBC patients treated with the anti-PD1 Pembrolizumab (Keytruda; Merck; NCT01848834), and the anti-PD-L1 Atezolizumab (Tecentriq; Roche). Moreover, xCT targeting could be successfully coupled with chemotherapy, since many chemotherapeutic drugs eliminate differentiated cancer cells but expand CSCs by inducing a hypoxia-inducible factor (HIF)-1-dependent increase in xCT, leading to increased GSH and subsequent mitogen-activated protein kinase (MEK) inhibition and Foxo3 activation, which induces the transcription of Nanog and other stem-cell related genes.⁵⁴ In fact, we have previously demonstrated that combining anti-xCT DNA vaccination with doxorubicin significantly enhanced the anti-metastatic potential of the single treatments.⁷ Since different signaling and metabolic pathways contribute to the maintenance of CSC phenotype and CSCs present a high degree of plasticity,⁴ another intriguing possibility would be a combination of multiple CSC-directed therapies to improve CSC elimination and prevent resistant clone onset. Using xCT immunotherapy together with metformin, a drug used to treat type 2 diabetes currently undergoing clinical trials in breast cancer patients, may exert a synergistic effect as xCT inhibition fosters the tricarboxylic acid (TCA) cycle by increasing intracellular glutamate levels, making cancer cells more resistant to glucose starvation.¹⁰

This negative effect can be hindered by metformin's inhibition of the TCA cycle and mitochondrial respiration.⁵⁵

In conclusion, we have demonstrated that xCT immune-targeting via BoHV-4 based vectors is a safe strategy with which to target mammary CSCs and impair tumor growth and metastatic spread, making it a potential candidate for the further development of combination therapies that aim to prevent recurrence in breast cancer patients.

Materials and methods

Cell and tumorsphere cultures

4T1 and SKBR3 cells were purchased from ATCC. TUBO cells were cultured as in.²⁷ Cells tested negative for mycoplasma⁵⁶ were passaged for fewer than 6 months. Tumorspheres were generated as in,²⁷ and used at the second passage (P2), except where otherwise specified. Bovine embryo kidney cells (BEK), were provided by Dr. M. Ferrari, Istituto Zooprofilattico Sperimentale, Brescia, Italy; (BS CL-94). BEK cells that expressed cre recombinase (BEKcre), and HEK293T cells were cultured as in.³²

Generation of BoHV-4-mxCT

See Supplementary methods for details. Briefly, synthetic *Mouse* xCT ORF was amplified from SLC7a11 pDREAM 2.1 (GenScript), via PCR and cloned into the pIgKE2BVD3gD₁₀₆ intermediate shuttle vector to generate CMV-mxCTgD₁₀₆ and then into pINT2-CMV-mxCTgD₁₀₆. EcoRI-linearized pINT2-CMV-mxCTgD₁₀₆ was used for heat-inducible homologous recombination in SW102 *E. coli* that contained the pBAC-BoHV-4-A-TK-KanaGalK-TK genome targeted to the TK locus with the KanaGalK selector cassette, as in.³⁷ Selected SW102 *E. coli* clones carrying pBAC-BoHV-4 recombinants were analyzed using *HindIII* restriction enzyme digestion and Southern blotting with a probe directed to the mxCT sequence.⁵⁷ BAC DNA (5 µg), was electroporated into BEK and BEKcre cells which were left to grow until the cytopathic effect (CPE), appeared. BoHV-4-mxCT and control BoHV-4-A29 were propagated by infecting BEK. Once CPE affected the majority of the cells, the virus was prepared by freezing and thawing cells three times before the virions were pelleted, using a 30% sucrose cushion,⁵⁸ and then resuspended in EMEM.

FACS analysis

umorsphere-derived cells were stained using the Aldefluor kit (Stem Cell Technologies),⁴² or with anti-H-2Kd-FITC, anti-Fas-PE/Cy7 (BD Bioscience), and anti-MHC class II-APC (Miltenyi Biotec) as in.⁴² ROS content was measured using 2',7'-dihydrochlorofluorescein diacetate (DHCF-DA, Sigma-Aldrich).⁷ Cells were incubated with 100µg/ml RNase A and 50µg/ml propidium iodide (Sigma-Aldrich) for 30 min for cell cycle analysis.⁵⁹ For immune infiltrate investigations, single cell suspensions were derived from vaccinated mice lungs,⁶⁰ then stained with anti-CD45-VioGreen, anti-CD3-FITC, anti-CD4-APC/Vio770, anti-CD8-VioBlue, anti-CD49b-PE, anti-PD1-APC, anti-F4/80-PE/Vio770, anti-CD11b-FITC, anti-Ly6G-VioBlue, anti-Ly6C-APC/Vio770 (Miltenyi Biotec),

anti-CD69-PE/Vio770 (Biolegend), and anti-PDL1-PE (BD Bioscience), as in.⁶¹ Samples were acquired on a BD FACSVerser and analyzed using BD FACSSuite software.

CD107 degranulation and IFN- γ production assay

4T1 cells were incubated with 50 μ g/ml Mitomycin C (Sigma-Aldrich), at 37°C for 2 hours, then washed 4 times and cultured overnight or for 5 days in RPMI 10%FBS at 1×10^5 cells/well with 1×10^6 splenocytes recovered from untreated and vaccinated mice. In the last 4 hours, anti-CD107a/b-FITC Abs (BD Bioscience), and 10 μ g/ml brefeldin A (Sigma-Aldrich), were added. Cells were stained for surface antigens, fixed/permeabilized with the BD Cytofix/Cytoperm kit and stained with anti-IFN- γ -APC (BD Bioscience). Analyses were performed on CD45⁺-gated lymphocytes with subsequent gating on either CD4⁺ or CD8⁺. Gates were set on T lymphocytes that had not been treated with brefeldin A and FMO samples.⁶²

Immunofluorescence

Tumorspheres were cytospinned to glass slides and stained with mouse sera (1:50), as in,⁷ and nuclei were stained with DAPI (Sigma-Aldrich). Images were acquired on a TCS-SP5II confocal microscope and analyzed using LASAF software (Leica). Fluorescence was quantitated using ImageJ and integrated density was normalized to nuclei number.

ELISA assay

Antibody responses were evaluated on plates coated with either mouse xCT protein (Cloud-Clone Corp., 40 ng/well), human xCT protein (Abnova, 30 ng/well), or mouse xCT extracellular loop peptides (GenScript, 1 μ g/well). After blocking with 1% milk (Blotto, SantaCruz Biotechnology), for 2 hours at 37°C, mouse sera (1:50) were incubated for 2 hours at 37°C. A standard curve was generated for xCT proteins using a rabbit anti-xCT antibody (ThermoFisher). After 5 washes, HRP-conjugated-anti-mouse and anti-rabbit IgG Abs (Sigma-Aldrich; 1:2,000) were incubated for 1 hour at 37°C. TMB (Sigma-Aldrich) was added after 5 washes. The reaction was stopped using 2N HCl, and O.D. was measured at 450 nm using a 680XR microplate reader (BioRad).

Glutamate quantification

Glutamate was quantified in supernatants from 4T1 tumorspheres cultured for 5 days with mouse sera (1:50), or SASP or from 4T1 cells using the Amplex Red glutamic acid/glutamate oxidase assay kit (ThermoFisher), and was normalized to cell density.

ADCC

1×10^4 4T1 target cells were stained with 2 μ M CFSE (Molecular Probes), cultured overnight with untreated BALB/c mice splenocytes, used as effector cells (200:1, 100:1, and 50:1 E:T ratio), and vaccinated mice sera (1:50).

Cells were stained with 1 μ g/ml 7-AAD (BD Bioscience), and acquired using FACS. %ADCC for each serum was calculated as in.²⁵

In vitro cytotoxicity

1×10^4 CFSE-labelled 4T1 target cells were incubated with splenocytes from untreated or vaccinated mice as effector cells (200:1, 100:1, and 50:1 E:T ratio) for 48 hours, then harvested, stained with 1 μ g/ml 7-AAD, and acquired using FACS, as for ADCC.

Immune sera effects on tumorsphere formation

P1 tumorspheres were dissociated and either cultured with immunized mice sera (1:50), 50 μ M SASP or nothing. After 5 days, P2 tumorspheres were imaged using a ApoTome fluorescence microscope (Zeiss), and sphere diameter was measured using AxioVision 4.8 software.⁶³ Spheres were counted, dissociated and processed for FACS analysis.

RNA extraction and qPCR

Total RNA was isolated from TUBO and 4T1 tumorspheres after 5 days of incubation with mouse sera or SASP, and retrotranscribed to cDNA as in.²⁷ qPCR was performed with commercial Slc7a11 and Gapdh (QuantiTect Primer Assay; Qiagen), or Chac1 custom primers,⁸ as in.²⁷ Slc7a11 and exopression levels relative to spheres incubated with untreated sera were calculated, using the comparative $\Delta\Delta$ Ct method and expressed as fold change.

In vivo treatment

Female 6-week-old BALB/c mice (Charles River Laboratories) were maintained at the Molecular Biotechnology Center, University of Torino, in accordance with University Ethical Committee guidelines and European Directive 2010/63. Vaccination, performed before (preventive model), or after tumor challenge (therapeutic model), consisted of two i.p. injections of 10^6 TCID50 of either BoHV-4-A29 or BoHV-4-mxCT at a 2-week interval. Two weeks after the second vaccination, blood and spleens were collected from some mice, while others had 5×10^4 TUBO-tumorsphere derived cells injected i.v. and their lungs explanted 20 days later.⁷ In the T cell depletion experiment, mice were treated i.p. with PBS or 200 μ g of anti-CD4 (clone GK1.5), anti-CD8 (clone 53-6.72) or isotype control antibodies (all from Bioxcell) every 3 days starting from cell challenge. In the therapeutic model, 1×10^4 4T1 tumorsphere-derived cells were injected s.c. and the mice were vaccinated when the tumor had reached 2 mm mean diameter. s.c. tumor growth was reported as tumor volume. Mice were euthanized 20 days after cell challenge and lungs were removed.⁷ Right lungs were fixed in 4% formaldehyde, paraffin embedded, sectioned and H&E stained. Slides were digitalized using a PanoramicDesk scanner and analyzed with PanoramicViewer1.15.4 (3D HISTECH).

Two sections of each lung were prepared. In order to avoid double counting of the same lesion, the average of the values obtained by analyzing the two sections was calculated and then reported. Metastases and total lung area were determined using PannoramicViewer and ImageJ, respectively. The remaining lobes were processed for FACS.

Statistical analysis

Student's *t*-test was used. Data are shown as mean \pm SEM unless otherwise stated. *P* < 0.05 was considered significant.

Disclosure of interest

The authors declare that no potential conflicts of interest exist

Funding

This work was supported by grants from the Italian Association for Cancer Research (IG 16724), Fondazione Ricerca Molinette Onlus, and by the University of Torino, Italy.

ORCID

Gaetano Donofrio  <http://orcid.org/0000-0002-8984-0377>

Roberto Ruiu  <http://orcid.org/0000-0002-0431-2656>

Elisabetta Bolli  <http://orcid.org/0000-0002-1550-2391>

Valeria Rolih  <http://orcid.org/0000-0003-3923-9476>

Laura Conti  <http://orcid.org/0000-0003-1780-098X>

Federica Cavallo  <http://orcid.org/0000-0003-4571-1060>

References

- Siegel RL, Miller KD, Jemal A. Cancer Statistics, 2017. *CA Cancer J Clin.* 2017;67:7–30. doi:10.3322/caac.21387.
- Colleoni M, Sun Z, Price KN, Karlsson P, Forbes JF, Thurlimann B, Gianni L, Castiglione M, Gelber RD, Coates AS, et al. Annual hazard rates of recurrence for breast cancer during 24 years of follow-up: results from the international breast cancer study group trials I to V. *J Clin Oncol.* 2016;34:927–935. doi:10.1200/JCO.2015.62.3504.
- Peitzsch C, Tyutyunnykova A, Pantel K, Dubrovska A. Cancer stem cells: the root of tumor recurrence and metastases. *Semin Cancer Biol.* 2017;44:10–24. doi:10.1016/j.semcancer.2017.02.011.
- Baccelli I, Trumpp A. The evolving concept of cancer and metastasis stem cells. *J Cell Biol.* 2012;198:281–293. doi:10.1083/jcb.201202014.
- Lollini PL, Cavallo F, De Giovanni C, Nanni P. Preclinical vaccines against mammary carcinoma. *Expert Rev Vaccines.* 2013;12:1449–1463. doi:10.1586/14760584.2013.845530.
- Conti L, Ruiu R, Barutello G, Macagno M, Bandini S, Cavallo F, et al. Microenvironment, oncoantigens, and antitumor vaccination: lessons learned from BALB-neuT mice. *Biomed Res Int.* 2014;2014:534969. doi:10.1155/2014/534969.
- Lanzardo S, Conti L, Rooke R, Ruiu R, Accart N, Bolli E, et al. Immunotargeting of antigen xCT attenuates stem-like cell behavior and metastatic progression in breast cancer. *Cancer Res.* 2016;76:62–72. doi:10.1158/0008-5472.CAN-15-1208.
- De La Ballina LR, Cano-Crespo S, Gonzalez-Munoz E, Bial S, Estrach S, Cailleteau L, et al. Amino acid transport associated to cluster of differentiation 98 heavy chain (CD98hc) is at the crossroad of oxidative stress and amino acid availability. *J Biol Chem.* 2016;291:9700–9711. doi:10.1074/jbc.M115.704254.
- Conrad M, Sato H. The oxidative stress-inducible cystine/glutamate antiporter, system x (c) (-): cystine supplier and beyond. *Amino Acids.* 2012;42:231–246. doi:10.1007/s00726-011-0867-5.
- Shin CS, Mishra P, Watrous JD, Carelli V, D'Aurelio M, Jain M, et al. The glutamate/cystine xCT antiporter antagonizes glutamine metabolism and reduces nutrient flexibility. *Nat Commun.* 2017;8:15074. doi:10.1038/ncomms15074.
- Timmerman LA, Holton T, Yuneva M, Louie RJ, Padro M, Daemen A, et al. Glutamine sensitivity analysis identifies the xCT antiporter as a common triple-negative breast tumor therapeutic target. *Cancer Cell.* 2013;24:450–465. doi:10.1016/j.ccr.2013.08.020.
- Lo M, Wang YZ, Gout PW. The x(c)- cystine/glutamate antiporter: a potential target for therapy of cancer and other diseases. *J Cell Physiol.* 2008;215:593–602. doi:10.1002/jcp.21366.
- Sugano K, Maeda K, Ohtani H, Nagahara H, Shibutani M, Hirakawa K. Expression of xCT as a predictor of disease recurrence in patients with colorectal cancer. *Anticancer Res.* 2015;35:677–682.
- Cohen AS, Khalil FK, Welsh EA, Schabath MB, Enkemann SA, Davis A, et al. Cell-surface marker discovery for lung cancer. *Oncotarget.* 2017;8:113373–113402. doi:10.18632/oncotarget.23009.
- Zhang L, Huang Y, Ling J, Zhuo W, Yu Z, Luo Y, et al. Overexpression of SLC7A11: a novel oncogene and an indicator of unfavorable prognosis for liver carcinoma. *Future Oncol.* 2018. doi:10.2217/fo-2017-0540.
- Nagano O, Okazaki S, Saya H. Redox regulation in stem-like cancer cells by CD44 variant isoforms. *Oncogene.* 2013;32:5191–5198. doi:10.1038/onc.2012.638.
- Hasegawa M, Takahashi H, Rajabi H, Alam M, Suzuki Y, Yin L, et al. Functional interactions of the cystine/glutamate antiporter, CD44v and MUC1-C oncoprotein in triple-negative breast cancer cells. *Oncotarget.* 2016;7:11756–11769. doi:10.18632/oncotarget.7598.
- Chen RS, Song YM, Zhou ZY, Tong T, Li Y, Fu M, et al. Disruption of xCT inhibits cancer cell metastasis via the caveolin-1/beta-catenin pathway. *Oncogene.* 2009;28:599–609. doi:10.1038/onc.2008.414.
- Chen L, Li X, Liu L, Yu B, Xue Y, Liu Y. Erastin sensitizes glioblastoma cells to temozolomide by restraining xCT and cystathionine-gamma-lyase function. *Oncol Rep.* 2015;33:1465–1474. doi:10.3892/or.2015.3712.
- Ma MZ, Chen G, Wang P, Lu WH, Zhu CF, Song M, et al. Xc-inhibitor sulfasalazine sensitizes colorectal cancer to cisplatin by a GSH-dependent mechanism. *Cancer Lett.* 2015;368:88–96. doi:10.1016/j.canlet.2015.07.031.
- Weber CK, Liptay S, Wirth T, Adler G, Schmid RM. Suppression of NF-kappaB activity by sulfasalazine is mediated by direct inhibition of IkappaB kinases alpha and beta. *Gastroenterology.* 2000;119:1209–1218.
- Dillman RO. Is there a role for therapeutic cancer vaccines in the age of checkpoint inhibitors? *Hum Vaccin Immunother.* 2017;13:528–532. doi:10.1080/21645515.2016.1244149.
- Wong KK, Li WA, Mooney DJ, Dranoff G. Advances in Therapeutic Cancer Vaccines. *Adv Immunol.* 2016;130:191–249. doi:10.1016/bs.ai.2015.12.001.
- Lollini PL, De Giovanni C, Pannellini T, Cavallo F, Forni G, Nanni P. Cancer immunoprevention. *Future Oncol.* 2005;1:57–66. doi:10.1517/14796694.1.1.57.
- Bolli E, O'Rourke JP, Conti L, Lanzardo S, Rolih V, Christen JM, et al. A Virus-Like-Particle immunotherapy targeting Epitope-Specific anti-xCT expressed on cancer stem cell inhibits the progression of metastatic cancer in vivo. *OncoImmunology.* 2017:e1408746. doi:10.1080/2162402X.2017.1408746.
- Jacca S, Rolih V, Quaglino E, Franceschi V, Tebaldi G, Bolli E, et al. Bovine herpesvirus 4-based vector delivering a hybrid rat/human HER-2 oncoantigen efficiently protects mice from

- autochthonous Her-2(+) mammary cancer. *Oncoimmunology*. 2016;5:e1082705. doi:10.1080/2162402X.2015.1082705.
27. Conti L, Lanzardo S, Arigoni M, Antonazzo R, Radaelli E, Cantarella D, et al. The noninflammatory role of high mobility group box 1/Toll-like receptor 2 axis in the self-renewal of mammary cancer stem cells. *FASEB J*. 2013;27:4731–4744. doi:10.1096/fj.13-230201.
 28. Capocefalo A, Franceschi V, Mertens PP, Castillo-Olivares J, Cavirani S, Di Lonardo E, et al. Expression and secretion of Bluetongue virus serotype 8 (BTV-8)VP2 outer capsid protein by mammalian cells. *J Virol Methods*. 2010;169:420–424. doi:10.1016/j.jviromet.2010.08.002.
 29. Donofrio G, Cavirani S, Simone T, Van Santen VL. Potential of bovine herpesvirus 4 as a gene delivery vector. *J Virol Methods*. 2002;101:49–61.
 30. Donofrio G, Sartori C, Franceschi V, Capocefalo A, Cavirani S, Taddei S, et al. Double immunization strategy with a BoHV-4-vectorialized secreted chimeric peptide BVDV-E2/BoHV-1-gD. *Vaccine*. 2008;26:6031–6042. doi:10.1016/j.vaccine.2008.09.023.
 31. Franceschi V, Capocefalo A, Cavirani S, Donofrio G. Bovine herpesvirus 4 glycoprotein B is indispensable for lytic replication and irreplaceable by VSVg. *BMC Vet Res*. 2013;9:6. doi:10.1186/1746-6148-9-18.
 32. Capocefalo A, Mangia C, Franceschi V, Jacca S, Van Santen VL, Donofrio G. Efficient heterologous antigen gene delivery and expression by a replication-attenuated BoHV-4-based vaccine vector. *Vaccine*. 2013;31:3906–3914. doi:10.1016/j.vaccine.2013.06.052.
 33. Donofrio G, Sartori C, Ravanetti L, Cavirani S, Gillet L, Vanderplasschen A, et al. Establishment of a bovine herpesvirus 4 based vector expressing a secreted form of the bovine viral diarrhoea virus structural glycoprotein E2 for immunization purposes. *BMC Biotechnol*. 2007;7:68. doi:10.1186/1472-6750-7-68.
 34. Franceschi V, Capocefalo A, Calvo-Pinilla E, Redaelli M, Mucignat-Caretta C, Mertens P, et al. Immunization of knockout alpha/beta interferon receptor mice against lethal bluetongue infection with a BoHV-4-based vector expressing BTV-8 VP2 antigen. *Vaccine*. 2011;29:3074–3082. doi:10.1016/j.vaccine.2011.01.075.
 35. Redaelli M, Franceschi V, Capocefalo A, D'Avella D, Denaro L, Cavirani S, et al. Herpes simplex virus type 1 thymidine kinase-armed bovine herpesvirus type 4-based vector displays enhanced oncolytic properties in immunocompetent orthotopic syngenic mouse and rat glioma models. *Neuro Oncol*. 2012;14:288–301. doi:10.1093/neuonc/nor219.
 36. Donofrio G, Franceschi V, Lovero A, Capocefalo A, Camero M, Losurdo M, et al. Clinical protection of goats against CpHV-1 induced genital disease with a BoHV-4-based vector expressing CpHV-1 gD. *PLoS One*. 2013;8:e52758. doi:10.1371/journal.pone.0052758.
 37. Warming S, Costantino N, Di C, Na J, Ng C. Simple and highly efficient BAC recombineering using galK selection. *Nucleic Acids Res*. 2005;33:e36. doi:10.1093/nar/gni035.
 38. Franceschi V, Parker S, Jacca S, Crump RW, Doronin K, Hembrador E, et al. BoHV-4-Based Vector Single Heterologous Antigen Delivery Protects STAT1(-/-) Mice from Monkeypoxvirus Lethal Challenge. *PLoS Negl Trop Dis*. 2015;9:e0003850. doi:10.1371/journal.pntd.0003850.
 39. Craig L, Sanschagrin PC, Rozek A, Lackie S, Kuhn LA, Scott JK. The role of structure in antibody cross-reactivity between peptides and folded proteins. *J Mol Biol*. 1998;281:183–201. doi:10.1006/jmbi.1998.1907.
 40. Charafe-Jauffret E, Ginestier C, Iovino F, Tarpin C, Diebel M, Esterni B, et al. Aldehyde dehydrogenase 1-positive cancer stem cells mediate metastasis and poor clinical outcome in inflammatory breast cancer. *Clin Cancer Res*. 2010;16:45–55. doi:10.1158/1078-0432.CCR-09-1630.
 41. Rolla S, Nicolo C, Malinarich S, Orsini M, Forni G, Cavallo F, et al. Distinct and non-overlapping T cell receptor repertoires expanded by DNA vaccination in wild-type and HER-2 transgenic BALB/c mice. *J Immunol*. 2006;177:7626–7633.
 42. Talerico R, Conti L, Lanzardo S, Sottile R, Garofalo C, Wagner AK, et al. NK cells control breast cancer and related cancer stem cell hematological spread. *Oncoimmunology*. 2017;6:e1284718. doi:10.1080/2162402X.2017.1284718.
 43. Sato H, Tamba M, Ishii T, Bannai S. Cloning and expression of a plasma membrane cystine/glutamate exchange transporter composed of two distinct proteins. *J Biol Chem*. 1999;274:11455–11458.
 44. Verna AE, Franceschi V, Tebaldi G, Macchi F, Menozzi V, Pastori C, et al. Induction of Antihuman C-C Chemokine Receptor Type 5 Antibodies by a Bovine Herpesvirus Type-4 Based Vector. *Front Immunol*. 2017;8:1402. doi:10.3389/fimmu.2017.01402.
 45. Fusella F, Secli L, Busso E, Krepelova A, Moiso E, Rocca S, et al. The IKK/NF-kappaB signaling pathway requires Morgana to drive breast cancer metastasis. *Nat Commun*. 2017;8:1636. doi:10.1038/s41467-017-01829-1.
 46. Park IA, Hwang SH, Song IH, Heo SH, Kim YA, Bang WS, et al. Expression of the MHC class II in triple-negative breast cancer is associated with tumor-infiltrating lymphocytes and interferon signaling. *PLoS One*. 2017;12:e0182786. doi:10.1371/journal.pone.0182786.
 47. Takeuchi A, Saito T. CD4 CTL, a Cytotoxic Subset of CD4(+) T Cells, Their Differentiation and Function. *Front Immunol*. 2017;8:194. doi:10.3389/fimmu.2017.00194.
 48. Ryoo IG, Lee SH, Kwak MK. Redox Modulating NRF2: A Potential Mediator of Cancer Stem Cell Resistance. *Oxid Med Cell Longev*. 2016;2016:2428153. doi:10.1155/2016/2428153.
 49. Fazzari J, Lin H, Murphy C, Ungard R, Singh G. Inhibitors of glutamate release from breast cancer cells; new targets for cancer-induced bone-pain. *Sci Rep*. 2015;5:8380. doi:10.1038/srep08380.
 50. Dornier E, Rabas N, Mitchell L, Novo D, Dhayade S, Marco S, et al. Glutaminolysis drives membrane trafficking to promote invasiveness of breast cancer cells. *Nat Commun*. 2017;8:2255. doi:10.1038/s41467-017-02101-2.
 51. Srivastava MK, Sinha P, Clements VK, Rodriguez P, Ostrand-Rosenberg S. Myeloid-derived suppressor cells inhibit T-cell activation by depleting cystine and cysteine. *Cancer Res*. 2010;70:68–77. doi:10.1158/0008-5472.CAN-09-2587.
 52. Sato H, Shiiya A, Kimata M, Maebara K, Tamba M, Sakakura Y, Makino N, Sugiyama F, Yagami K-I, Moriguchi T, et al. Redox imbalance in cystine/glutamate transporter-deficient mice. *J Biol Chem*. 2005;280:37423–37429. doi:10.1074/jbc.M506439200.
 53. Ruiu R, Rolih V, Bolli E, Barutello G, Riccardo F, Quaglino E, et al. Fighting breast cancer stem cells through the immunetargeting of the xCT cystine-glutamate antiporter. *Cancer Immunol Immunother*. 2018. doi:10.1007/s00262-018-2185-1.
 54. Lu H, Samanta D, Xiang L, Zhang H, Hu H, Chen I, et al. Chemotherapy triggers HIF-1-dependent glutathione synthesis and copper chelation that induces the breast cancer stem cell phenotype. *Proc Natl Acad Sci U S A*. 2015;112:E4600–9. doi:10.1073/pnas.1513433112.
 55. Hirsch HA, Iliopoulos D, Tsiichlis PN, Struhl K. Metformin selectively targets cancer stem cells, and acts together with chemotherapy to block tumor growth and prolong remission. *Cancer Res*. 2009;69:7507–7511. doi:10.1158/0008-5472.CAN-09-2994.
 56. Geninatti Crich S, Cadenazzi M, Lanzardo S, Conti L, Ruiu R, Alberti D, et al. Targeting ferritin receptors for the selective delivery of imaging and therapeutic agents to breast cancer cells. *Nanoscale*. 2015;7:6527–6533. doi:10.1039/c5nr00352k.
 57. Donofrio G, Franceschi V, Capocefalo A, Taddei S, Sartori C, Bonomini S, et al. Cellular targeting of engineered heterologous antigens is a determinant factor for bovine herpesvirus 4-based vaccine vector development. *Clin Vaccine Immunol*. 2009;16:1675–1686. doi:10.1128/CVI.00224-09.
 58. Donofrio G, Cavaggioni A, Bondi M, Cavirani S, Flammini CF, Mucignat-Caretta C. Outcome of bovine herpesvirus 4 infection following direct viral injection in the lateral ventricle of the mouse brain. *Microbes Infect*. 2006;8:898–904. doi:10.1016/j.micinf.2005.10.016.
 59. Durelli L, Conti L, Clerico M, Boselli D, Contessa G, Ripellino P, et al. T-helper 17 cells expand in multiple sclerosis and are

- inhibited by interferon-beta. *Ann Neurol.* 2009;65:499–509. doi:10.1002/ana.21652.
60. Macagno M, Bandini S, Stramucci L, Quaglino E, Conti L, Balmas E, et al. Multiple roles of perforin in hampering ERBB-2 (Her-2/neu) carcinogenesis in transgenic male mice. *J Immunol.* 2014;192:5434–5441. doi:10.4049/jimmunol.1301248.
 61. Bandini S, Macagno M, Hysi A, Lanzardo S, Conti L, Bello A, et al. The non-inflammatory role of C1q during Her2/neu-driven mammary carcinogenesis. *Oncoimmunology.* 2016;5:e1253653. doi:10.1080/2162402X.2016.1253653.
 62. Conti L, De Palma R, Rolla S, Boselli D, Rodolico G, Kaur S, et al. Th17 cells in multiple sclerosis express higher levels of JAK2, which increases their surface expression of IFN-gammaR2. *J Immunol.* 2012;188:1011–1018. doi:10.4049/jimmunol.1004013.
 63. Conti L, Lanzardo S, Ruiu R, Cadenazzi M, Cavallo F, Aime S, et al. L-Ferritin targets breast cancer stem cells and delivers therapeutic and imaging agents. *Oncotarget.* 2016;7:66713–66727. doi:10.18632/oncotarget.10920.